大質量ブラックホール降着円盤から放出される大強度アルフヴェンパルスとジェット

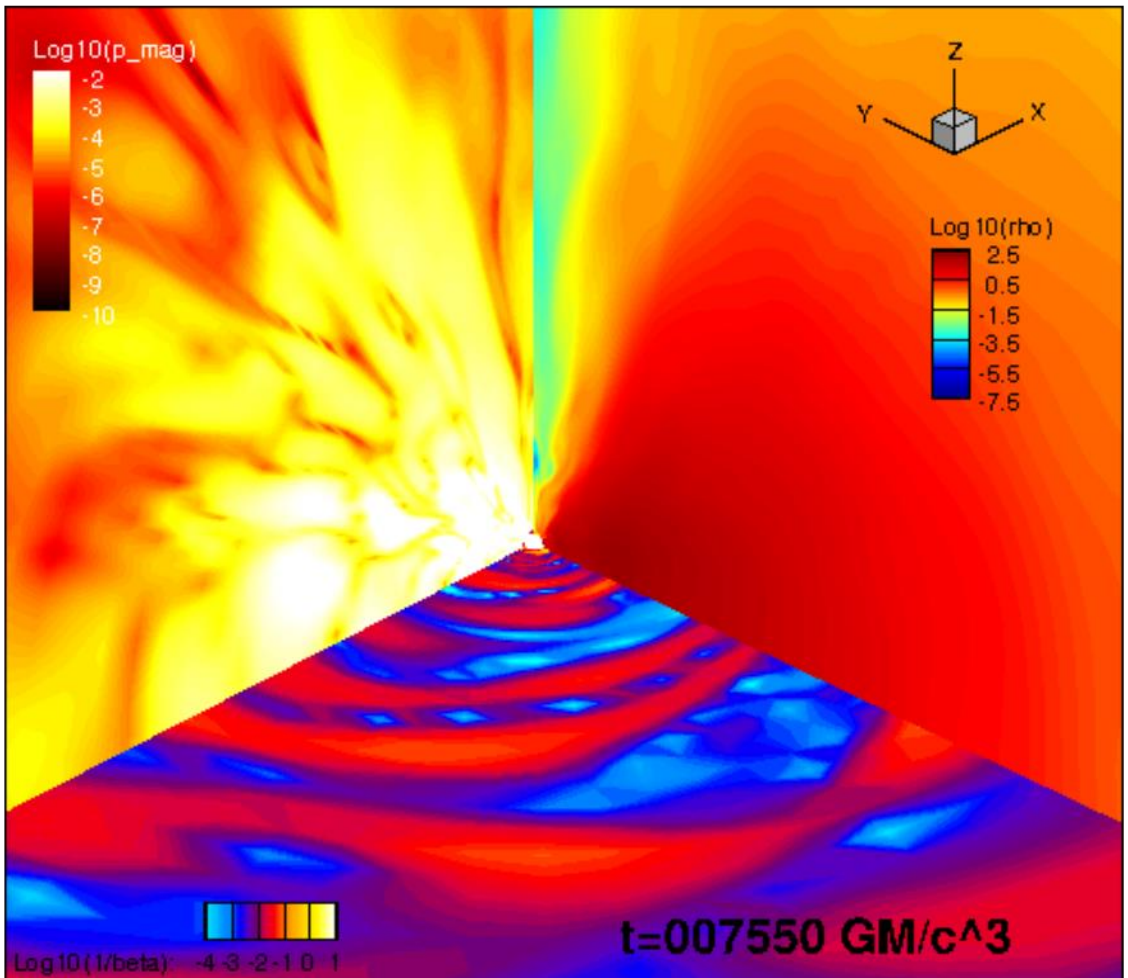

水田　晃(理化学研究所)

References

AM, Ebisuzaki Tajima Nagataki, MNRAS 479 2534(2018)

the case of spin a=0.9

AM+ in prep.

parameter study in spin a

CFCAユーザーズミーティング

@国立天文台(三鷹)

2019.01.15

Active Galactic Nuclei Jet

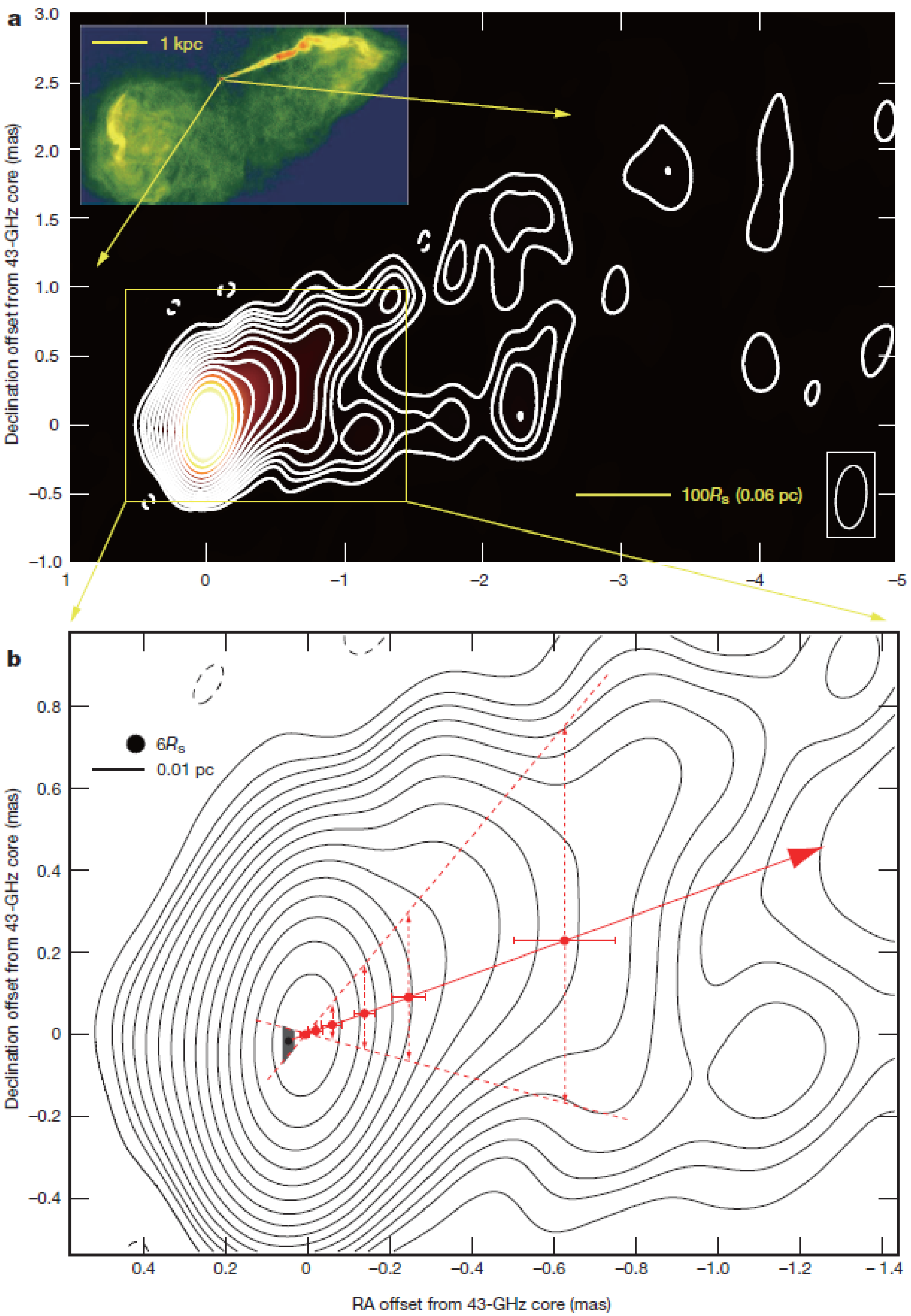

M87 radio observation Hada +(2011)

Hilghlly collimated outflows from center of galaxy

- central engine
  supermassive black hole
  +
  accretion disk
- relativistic outflows
  Bulk Lorentz factor : Γ ~ 10

- multiwavelength emission
  radio to high energy γ-rays

- strong candidate of
  ultra high energy cosmic ray accelerator
  via Fermi acc. ? (1954)
  wake field acc.
  (Ebisuzaki & Tajima 2014)

ブラックホール降着円盤とジェット形成

中心エンジン (Black Hole(BH)＋ disk)

-円盤の時間変動 (Shibata +1990, Balbus & Hawley1991)

-- MRI growth (B ↗ => Low beta state)

Magnetorotational instability(磁気回転不安定性)

– 差動回転： $d\Omega_{disk}$ /dr < 0

$\Omega_{disk} \propto r^{-1.5}$:Kepler rotation

– B ∝ exp (iωt) 指数関数的増幅

Unstable @ $0 < kV_a < 1.73\ \Omega_K$

Most unstable @ $kV_a \sim \Omega_K$ $\omega \sim 0.75\Omega_K$

– MRI によって角運動量輸送

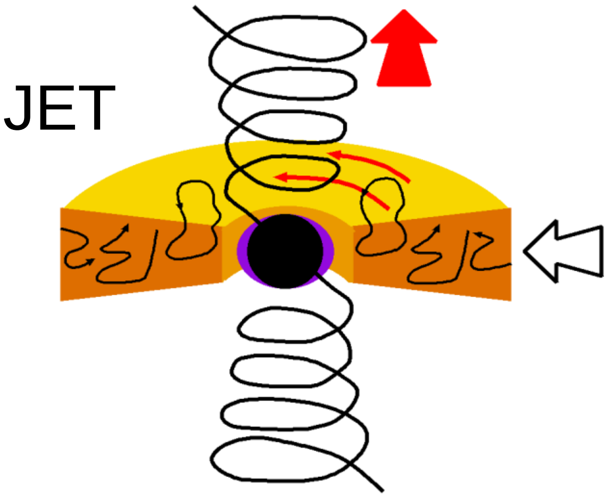

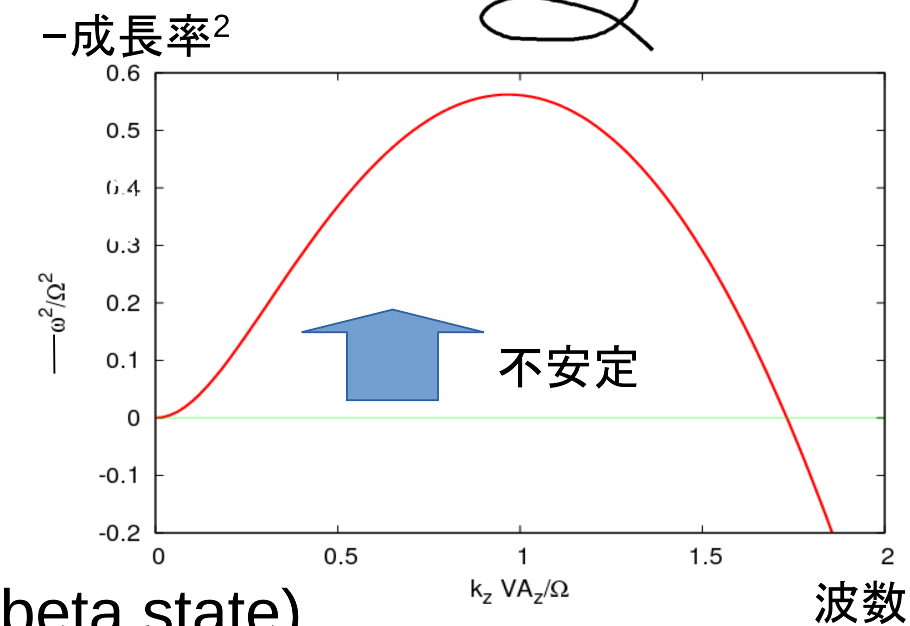

-- 磁気エネルギーの散逸 (B ↘=> High beta state)

-- 円盤鉛直方向に Strong Alfven burst (Low β => High β)
ジェット中を伝播し、wake field 加速機構による宇宙線の起源やブレーザー天体の短時間変動 (Ebisuzaki +2014, A.M2018)

Basic Equations : GRMHD Eqs.

GM=c=1, a: dimensionless Kerr spin parameter

$$\frac{1}{\sqrt{-g}}\partial_\mu(\sqrt{-g}\rho u^\mu) = 0$$ Mass conservation Eq.

$$\partial_\mu(\sqrt{-g}T^\mu_\nu) = \sqrt{-g}T^\kappa_\lambda \Gamma^\lambda{}_{\nu\kappa}$$ Energy-momentum conservation Eq.

$$\partial_t(\sqrt{-g}B^i) + \partial_j(\sqrt{-g}(b^i u^j - b^j u^i)) = 0$$ Induction Eq.

$$p = (\gamma - 1)\rho\epsilon$$ EOS (γ=4/3)

Constraint equations.

$$\frac{1}{\sqrt{-g}}\partial_i(\sqrt{-g}B^i) = 0$$ No-monopoles constraint

$$u_\mu b^\mu = 0$$ Ideal MHD condition

$$u_\mu u^\mu = -1$$ Normalization of 4-velocity

Energy-momentum tensor

$$T^{\mu\nu} = (\rho h + b^2)u^\mu u^\nu + (p_{\rm g} + p_{\rm mag})g^{\mu\nu} - b^\mu b^\nu$$

$$p_{\rm mag} = b^\mu b_\mu/2 = b^2/2$$

$$b^\mu \equiv \epsilon^{\mu\nu\kappa\lambda}u_\nu F_{\lambda\kappa}/2 \quad B^i = F^{*it}$$

GRMHD code (Nagataki 2009,2011)

Kerr-Schild metric (no singular at event horizon)

HLL flux, 2nd order in space (van Leer), 2nd or 3rd order in time

See also, Gammie +03, Noble + 2006

Flux-interpolated CT method for divergence free

Initial Condition

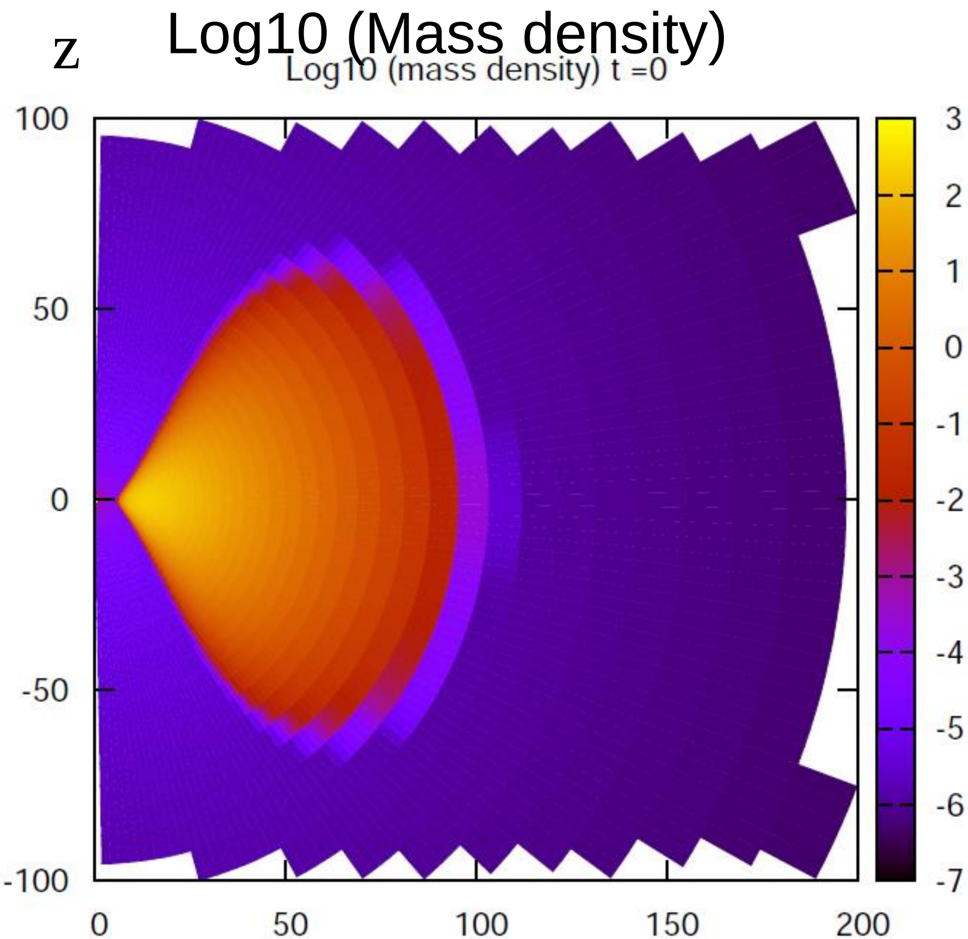

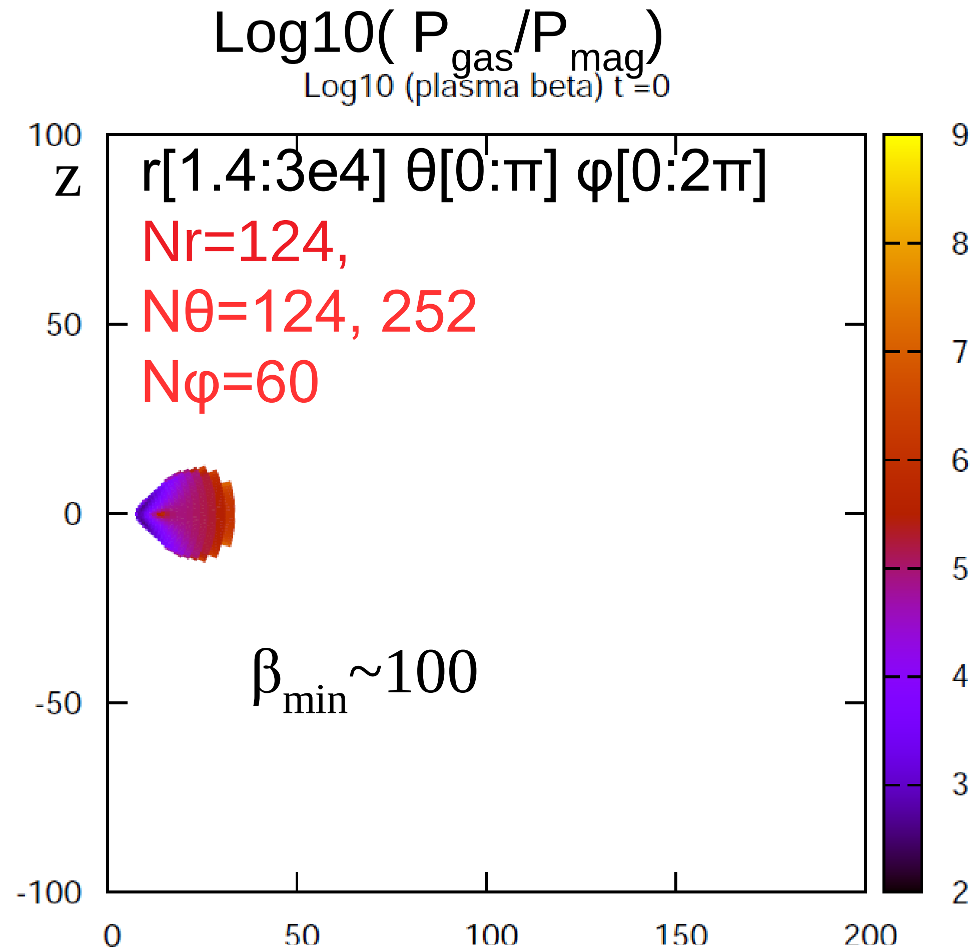

$$A_\phi \propto \max\left[\rho/\rho_{\max} - 0.2, 0\right]$$

Fisbone-Moncrief (1976) solution – hydrostatic solution of tori around rotating BH (**a=0.9**, rH~1.44), $l_* \equiv -u^t u_\phi$ =const =4.45, r_{in}=6. > r_{ISCO}

With maximum 5% random perturbation in thermal pressure.

Units L : Rg=GM/c^2 (=Rs/2), T : Rg/c=GM/c^3, mass : scale free

~1.5x10^{13}cm($M_{BH}/10^8 M_{sun}$) ~500s ($M_{BH}/10^8 M_{sun}$)

Grids to capture MRI fastest growing mode

Wavelength of fastest growing mode in the disk

$\lambda_{MRI} = 2\pi \langle C_{az} \rangle / \Omega_K (R) \sim 0.022 (R/R_{ISCO})^{1.5}$

$\langle C_s \rangle \sim \langle C_{A\,z} \rangle \sim 10^{-3}\, c$

$R_{ISCO}\,(a=0.9)=2.32$

$N_\theta = 252$

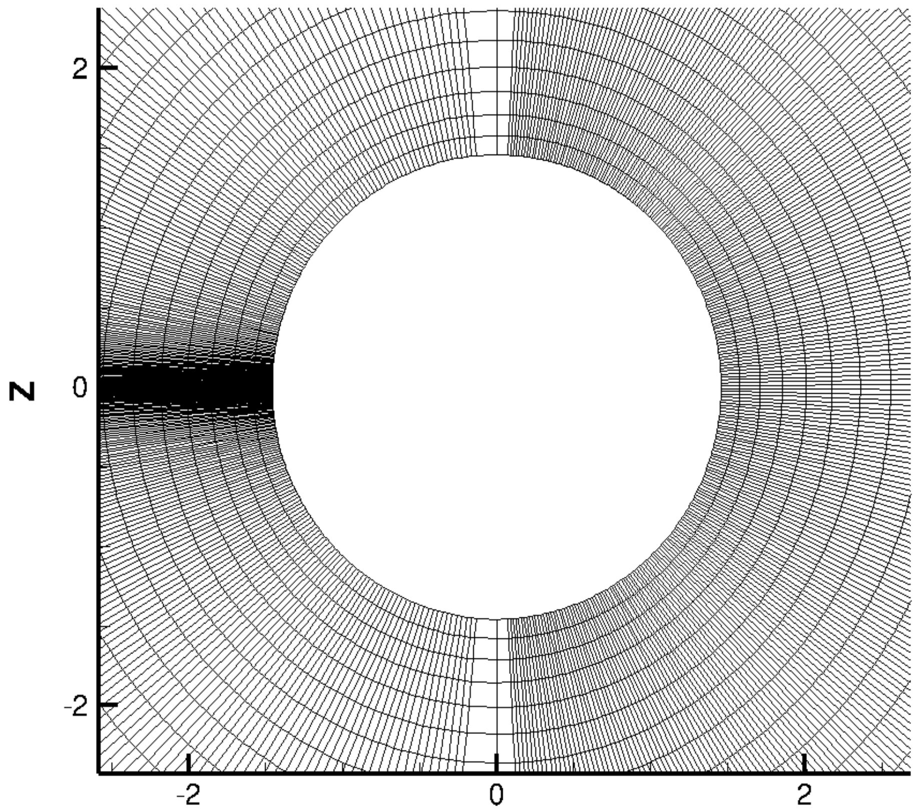

$$\theta = \pi x_2 + \frac{1}{2}(1-h)\sin(2\pi x_2)$$

$x_2 = [0:1]$ Δx_2=cost

h=0.2

$\Delta\theta$=cost

h=1

McKinney and Gammie

□□□□

Any coordinates described by analytic function can be applied (generalized curvilinear coordinates)

$$\theta_{KS}(\vartheta) = \vartheta + \frac{2h\vartheta}{\pi^2}(\pi - 2\vartheta)(\pi - \vartheta).$$

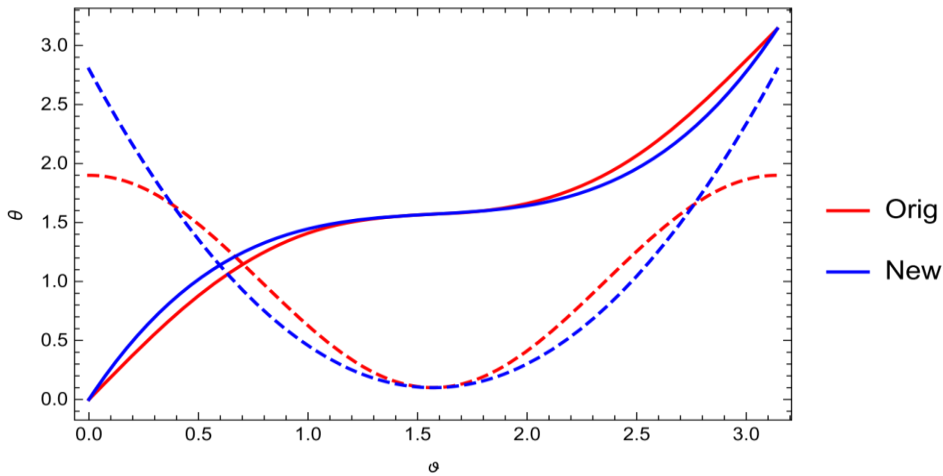

Porth + 2017

Higher resolution calculation in θ around equator

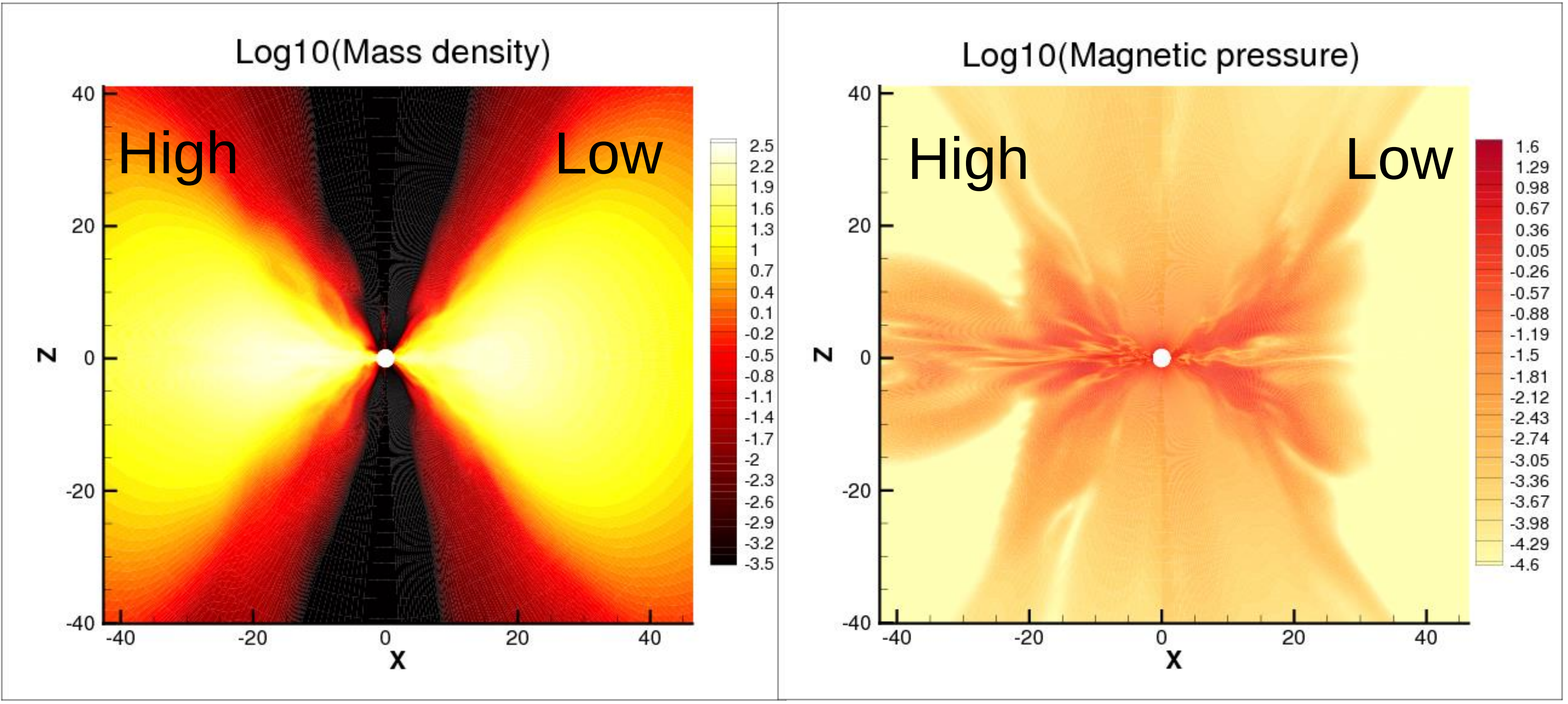

Right : about 8 times higher resolution in theta @ equator

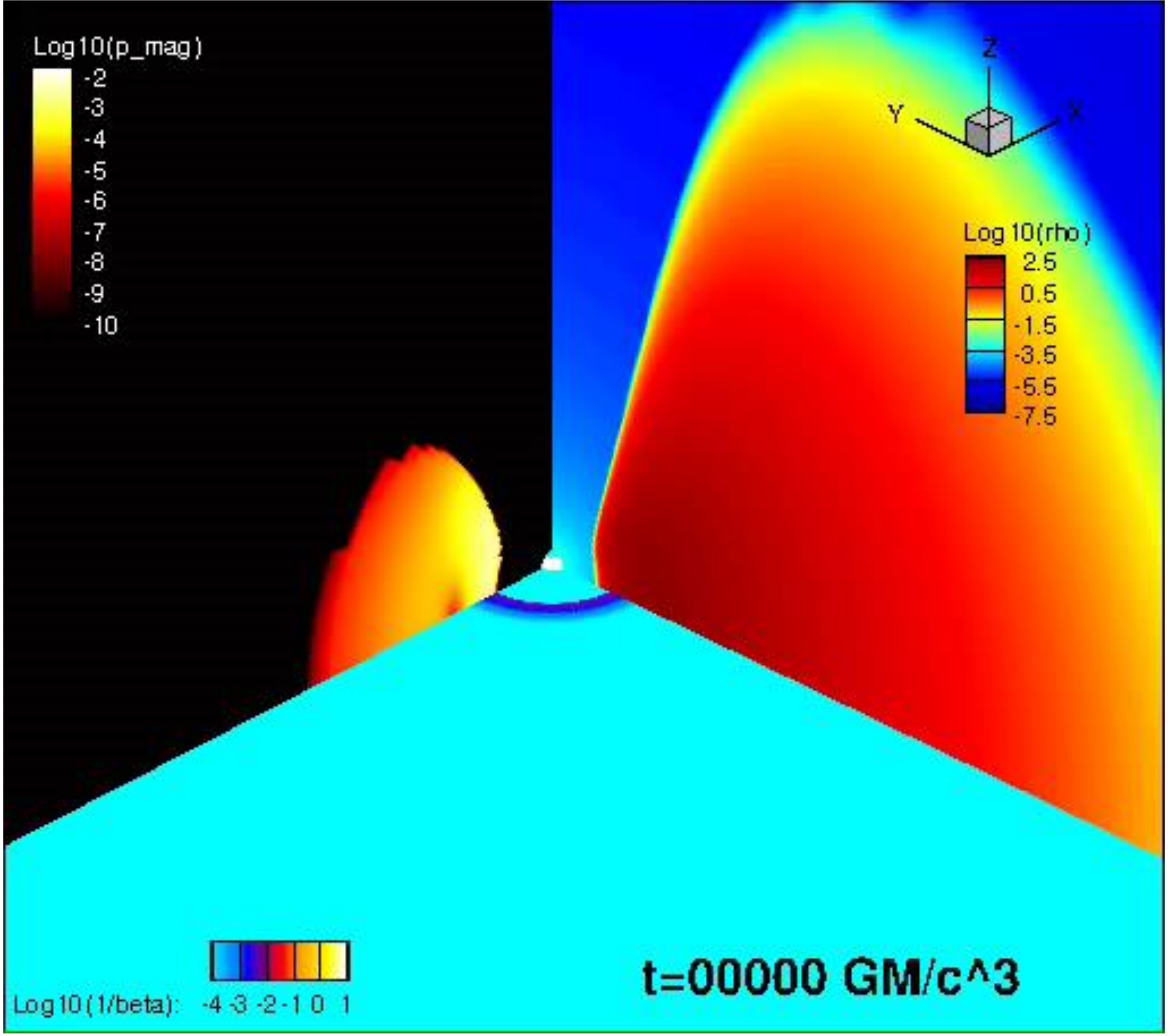

Disk : Fishbone Moncrief solution, spin parameter **a=0.9 (0.7, 0.5, 0.3, 0.1)**
spherical coordinate R[0.98 r_H (a):3e4] θ[0:π] φ[0:2π]
[NR=124,**Nθ=252, Nφ=60**] r=exp(n_r), θ :**non-niform (concentrate @ equator)**
dφ~6^o: uniform Poloidal B filed, β_min=100

B-filed amplification & mass accretion

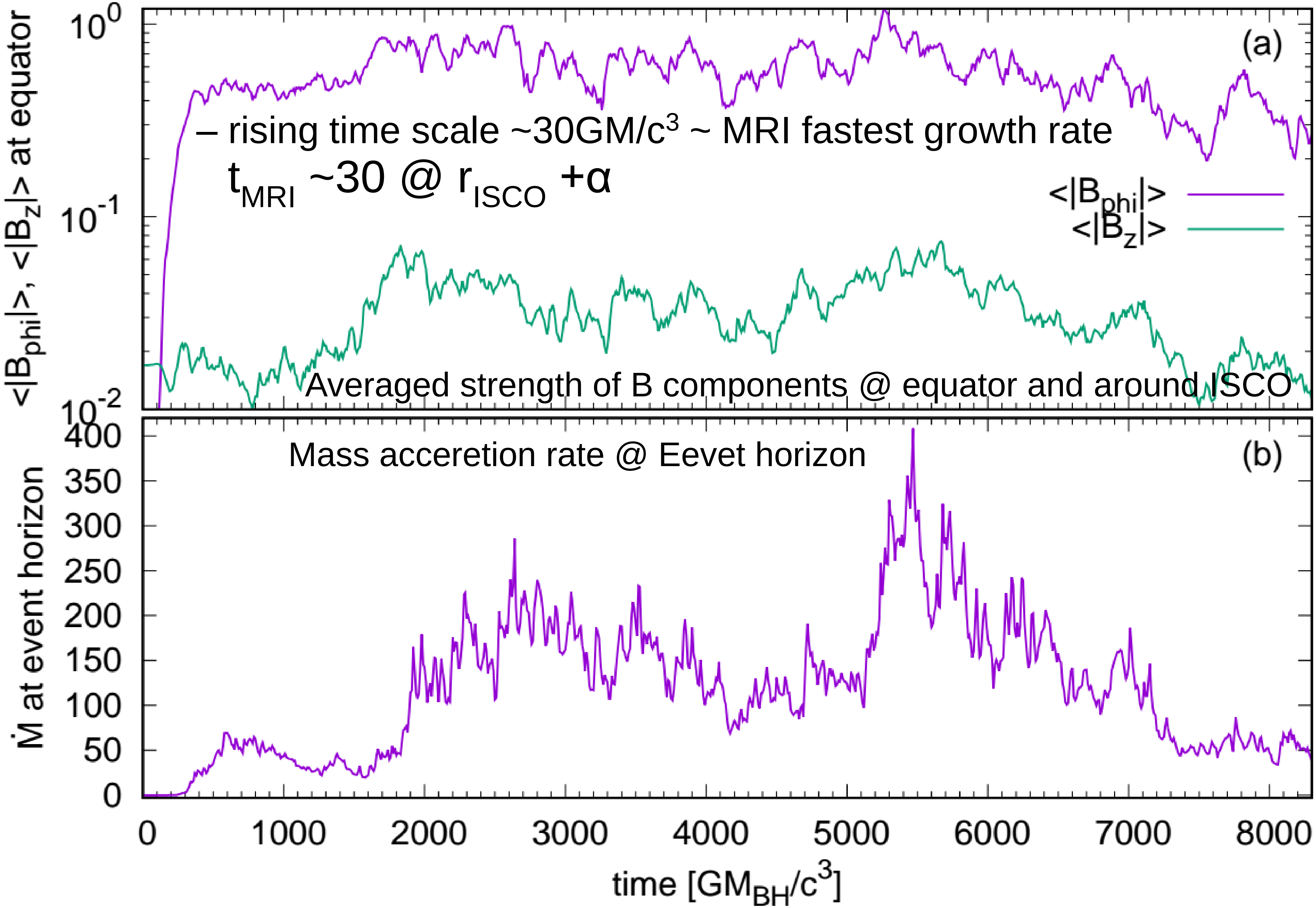

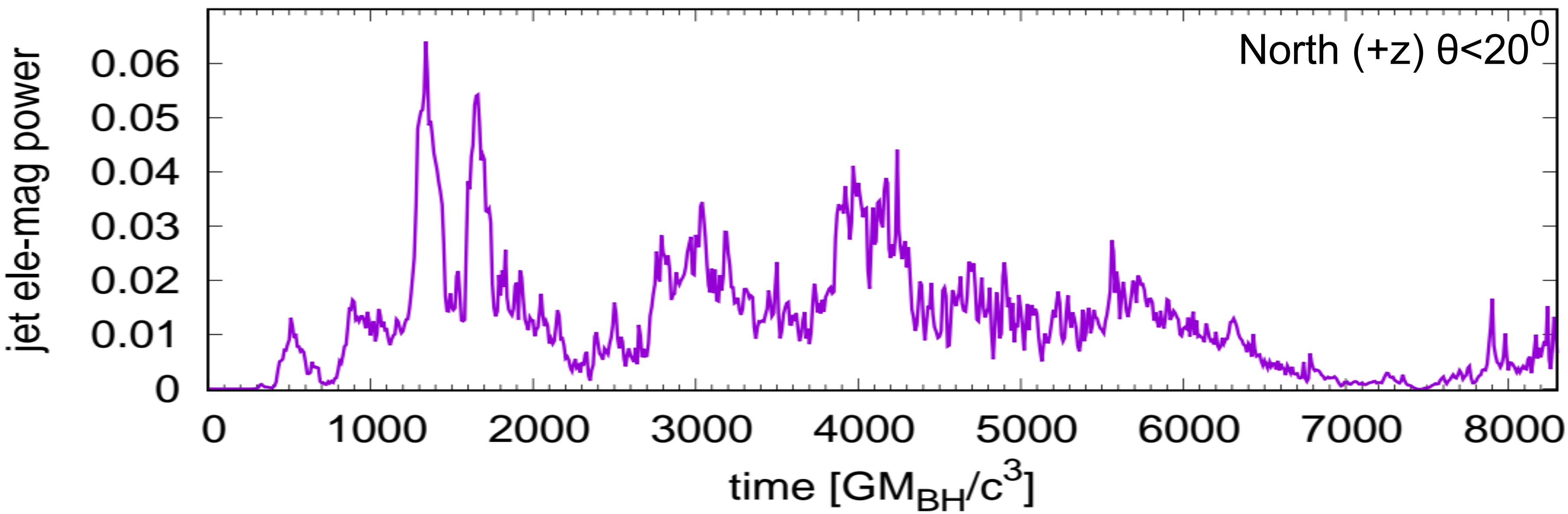
North (+z) θ<20⁰
jet ele-mag power
0.06
0.05
0.04
0.03
0.02
0.01
0
0
1000
2000
3000
4000
5000
6000
7000
8000
time [GM_BH/c^3]

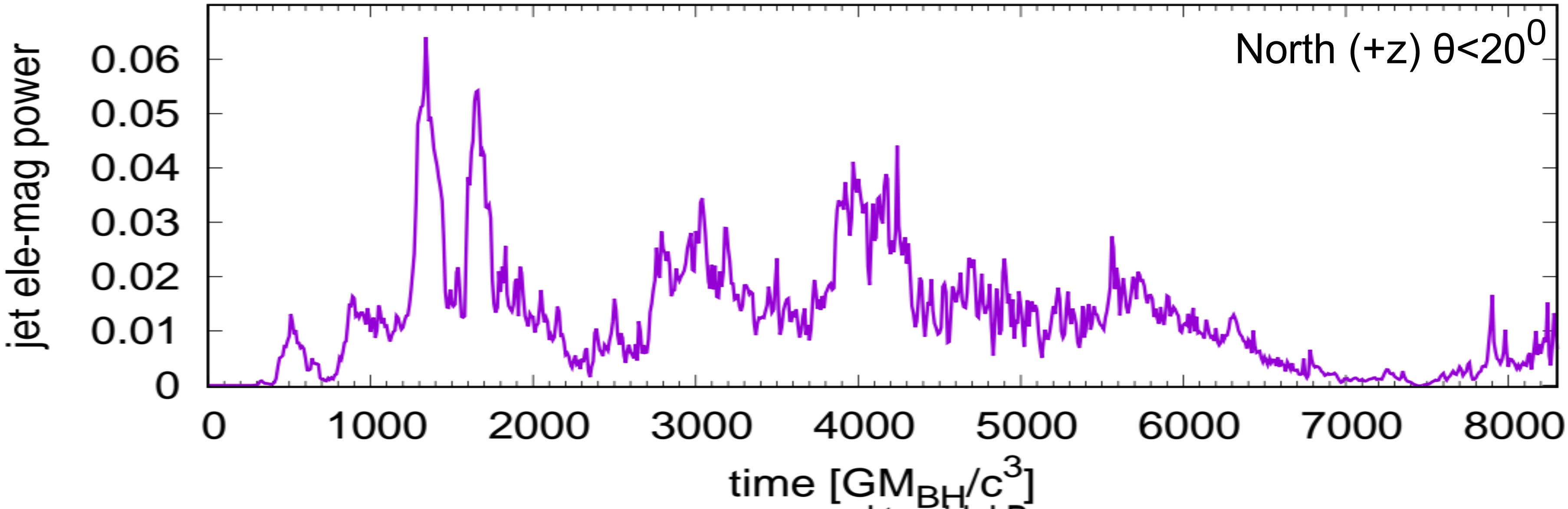

averaged toroidal B

<Bφ>@R=3Rg

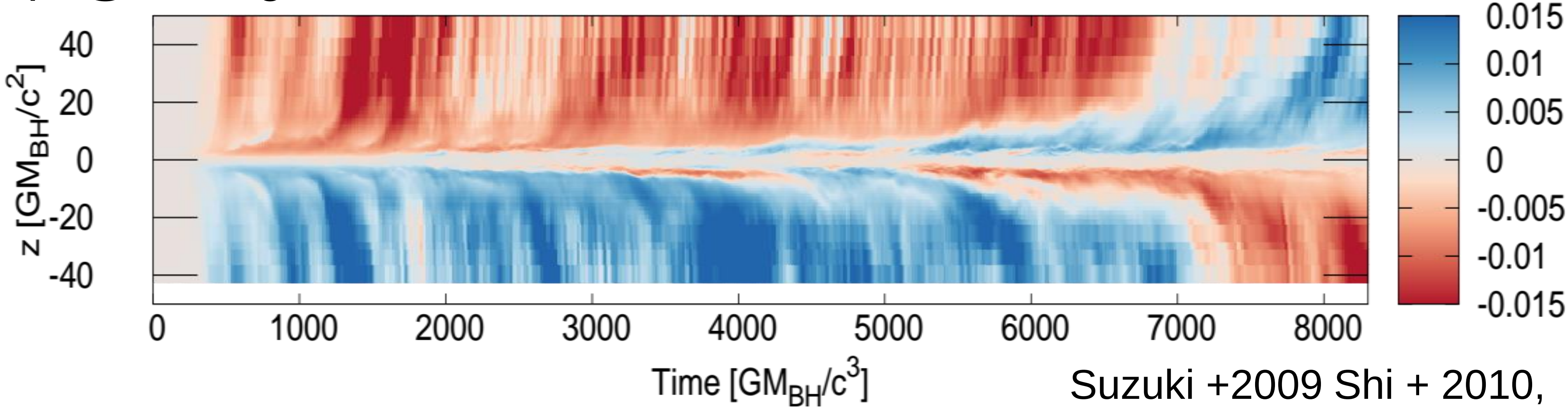

Suzuki +2009 Shi + 2010,
Machida +2013

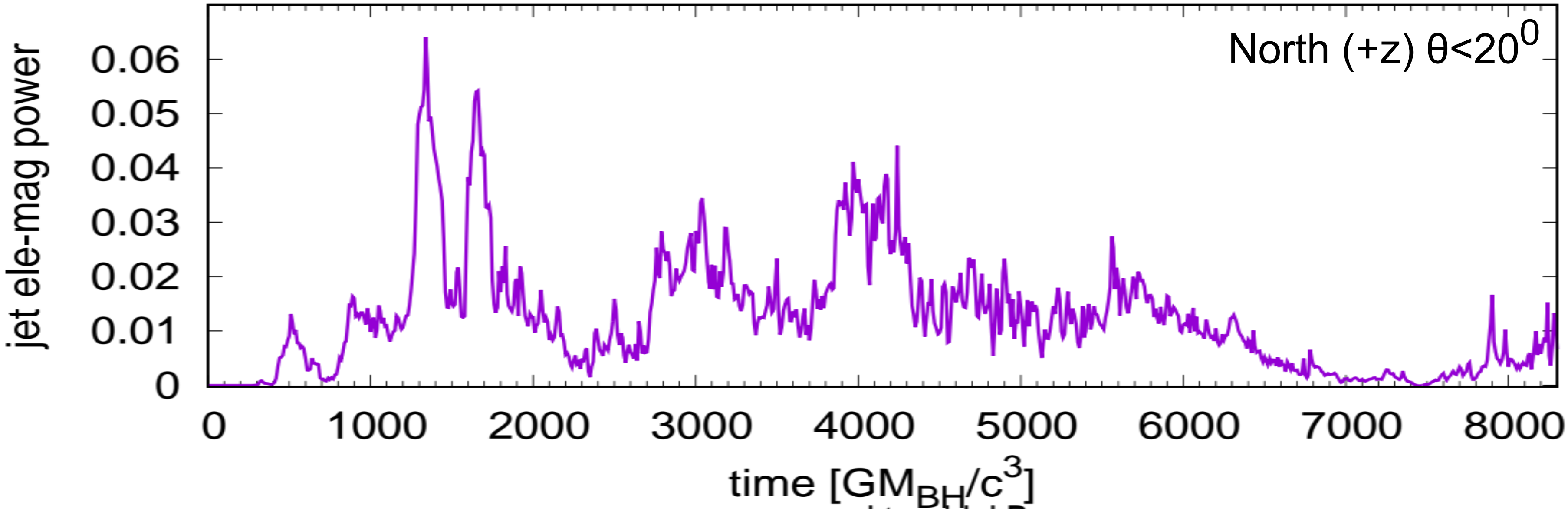

<Bφ>@R=3Rg

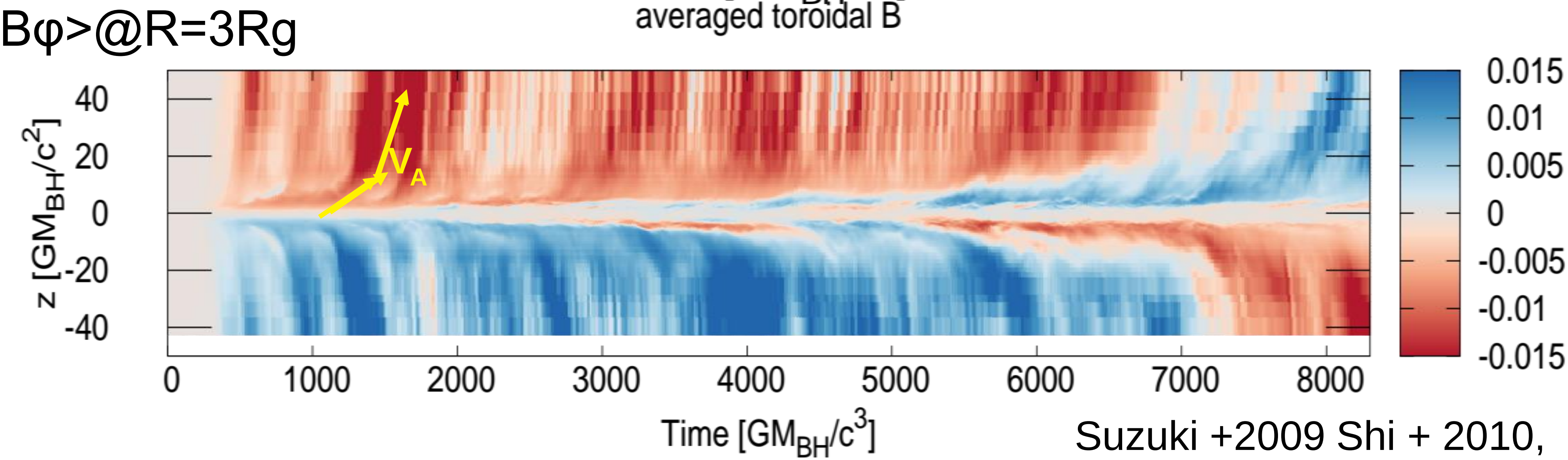

Suzuki +2009 Shi + 2010,
Machida +2013

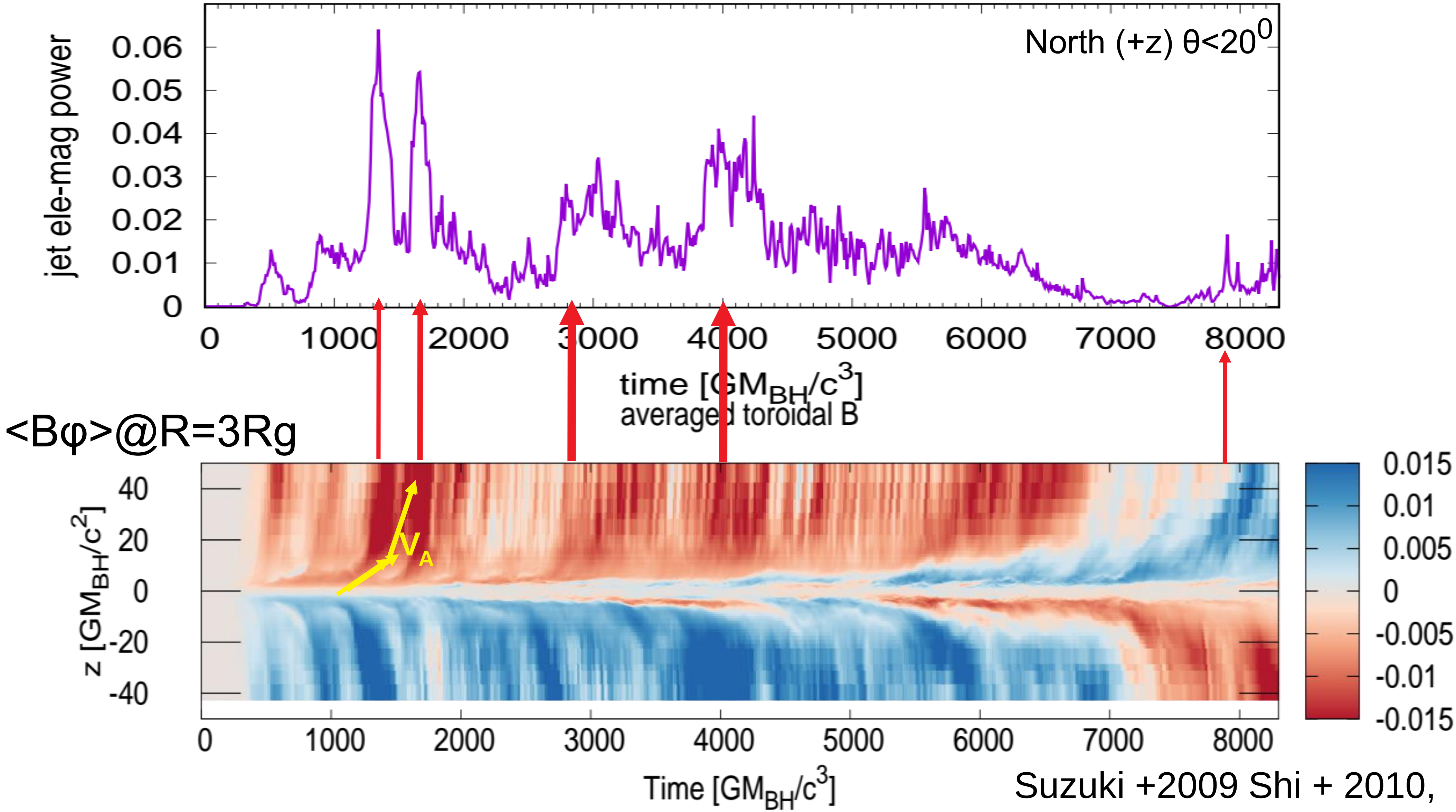

Suzuki +2009 Shi + 2010,
Machida +2013
Takasao+2018 =>後述

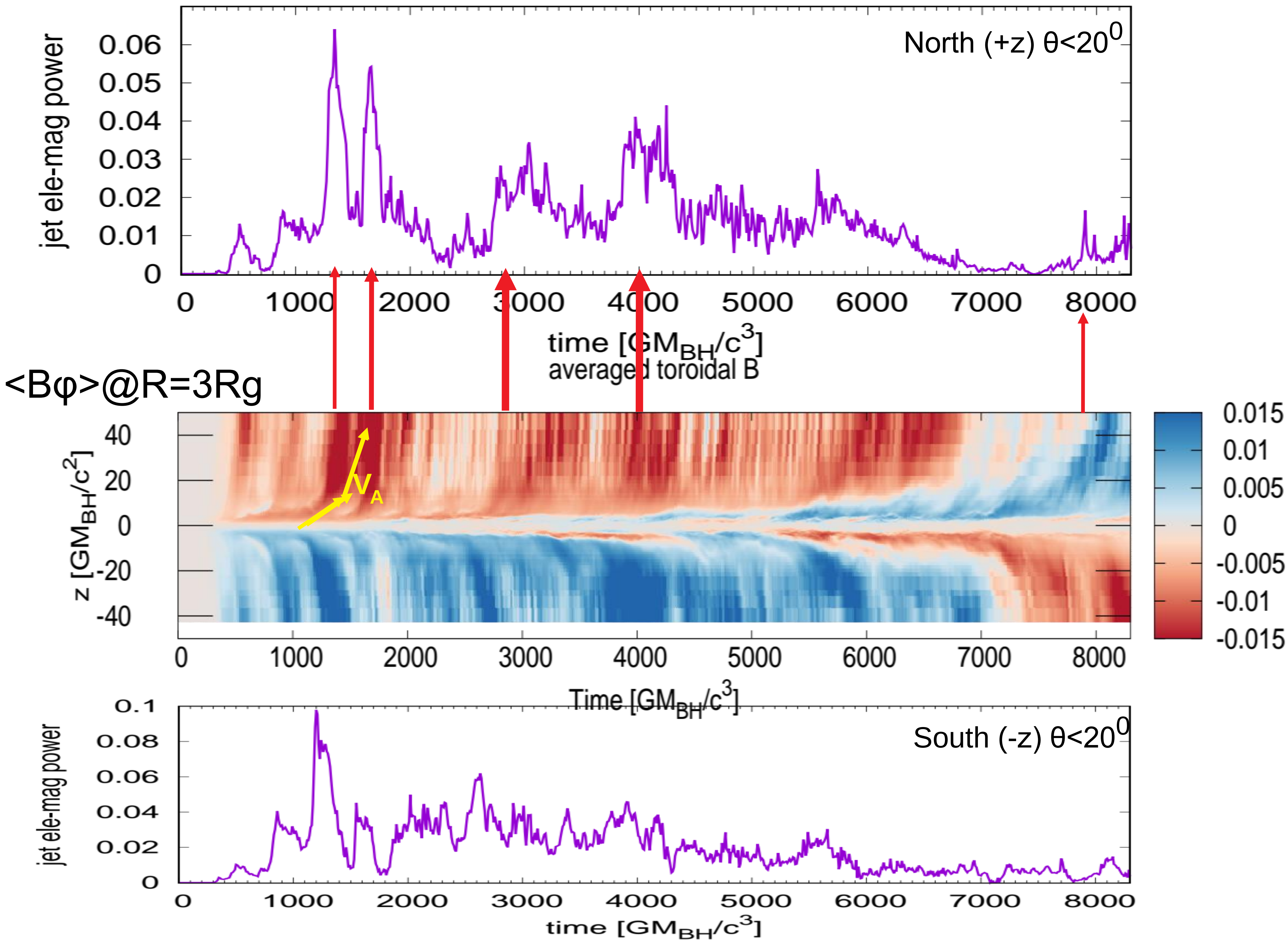
North (+z) θ<20^0
jet ele-mag power
time [GM_BH/c^3]
averaged toroidal B
<Bφ>@R=3Rg
V_A
z [GM_BH/c^2]
Time [GM_BH/c^3]
South (-z) θ<20^0
jet ele-mag power
time [GM_BH/c^3]

Butterfly diagram is common feature of accretion disk

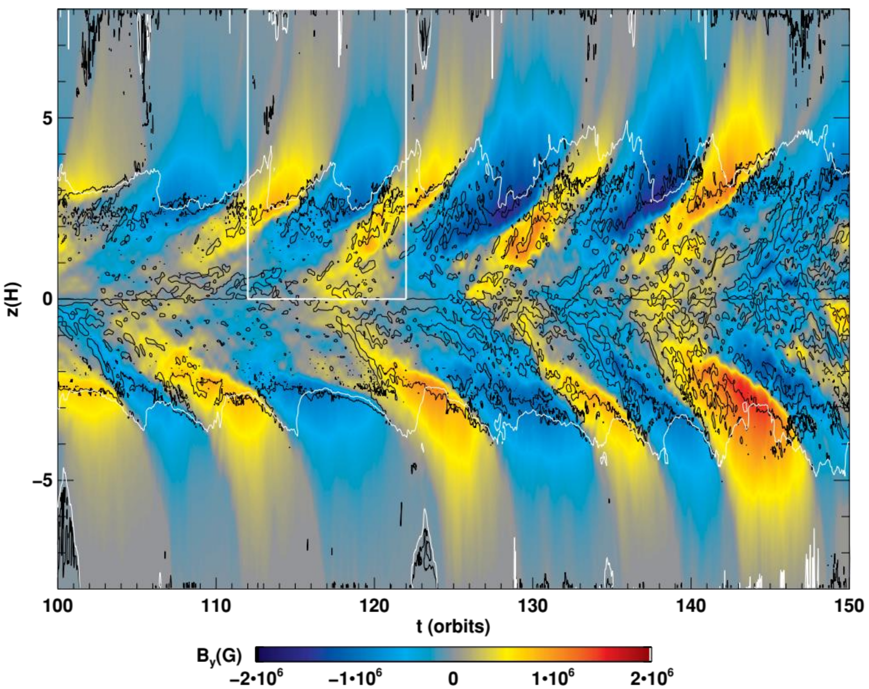

Shi + 2011
Local box sim.
Protosteller disk

繰り返し周期は
10回転周期程度
極性が変わる

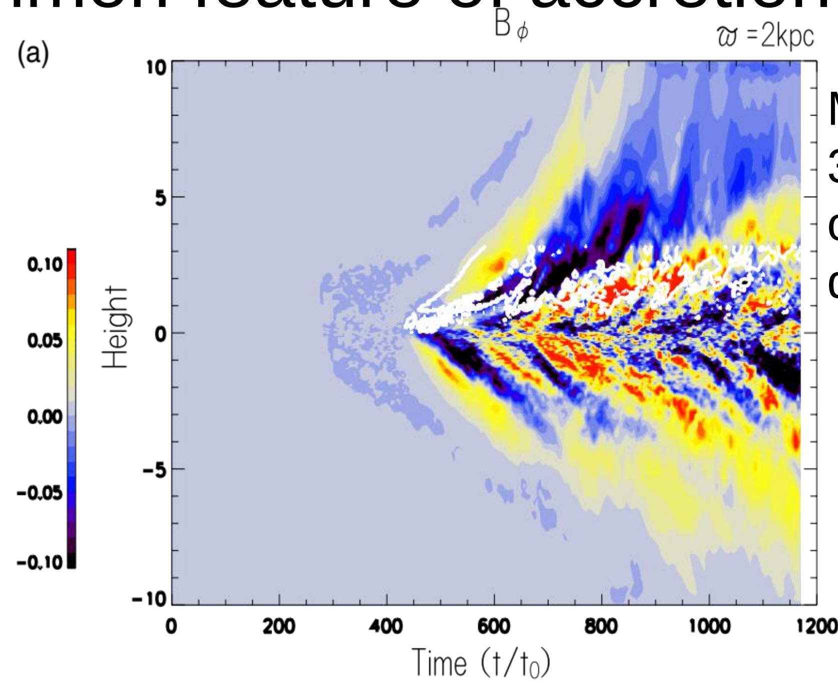

Machida + 2013
3D MHD sim
of galactic
dynamo

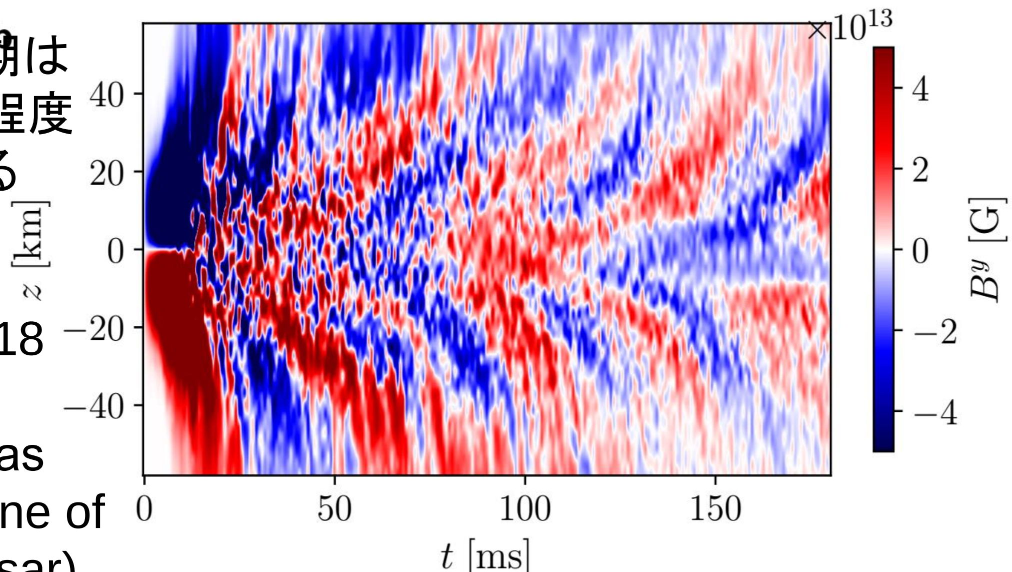

Siegel + 2018
GRMHD
+ ν cooling as
central engine of
GRB(collapsar)

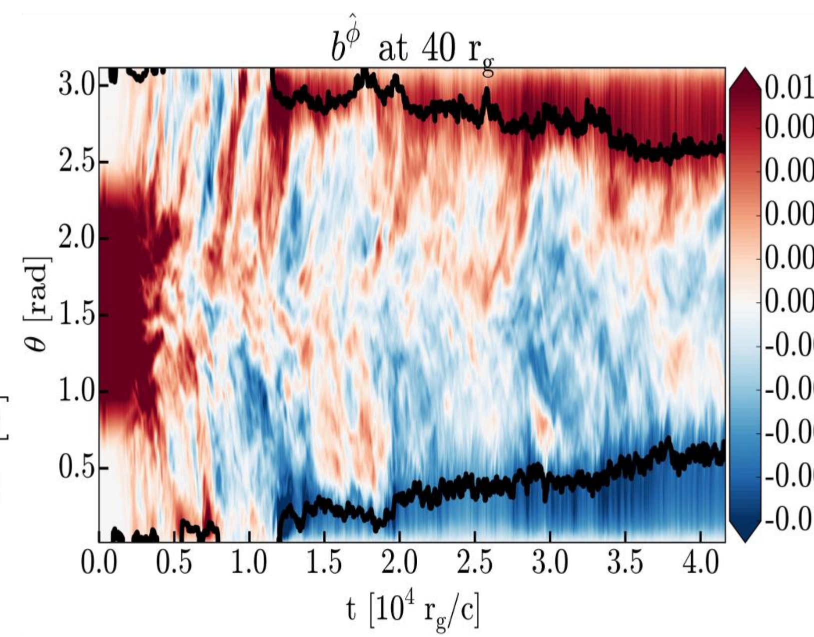

Liska + 2018
GRMHD+AMR

Event horizon / ISO(innermost stable circular orbit)

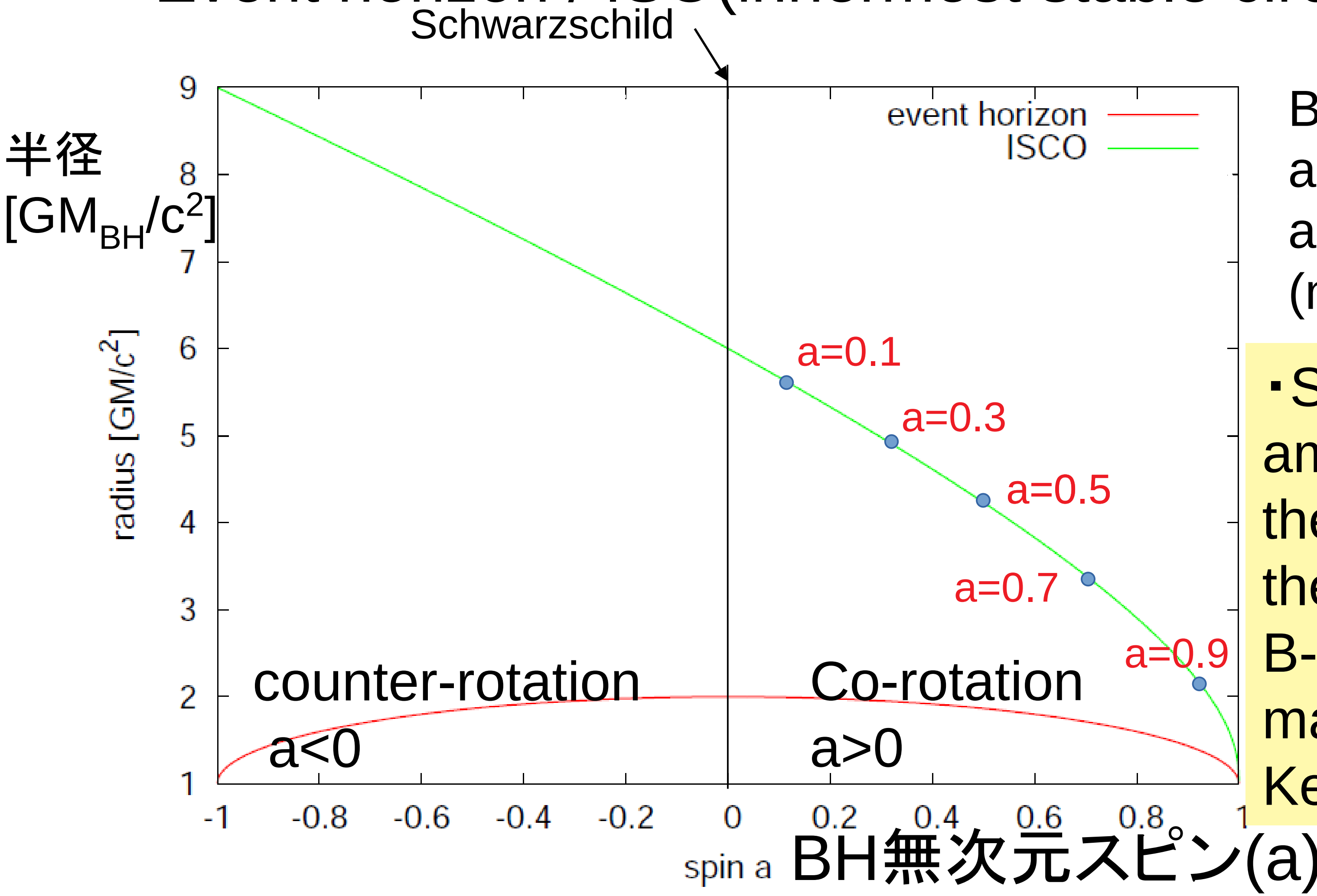

Both r_H and r_{ISCO} approaches r=1 as a=> 1 (maximum spin)

・Since B-field amplification occurs in the disk (r>r_ISCO), the timescale of B-filed amplification may depends on Kerr-spin parameter.

$$r_{\rm H} = 1 + \sqrt{1 - a^2}$$ (g_{rr} =0 @ Boyer-Lindquist)

$$r_{\rm ISCO} = 3 + g(a) \mp \sqrt{[3 - f(a)][3 + f(a) + 2g(a)]}$$

$$f(a) \equiv 1 + (1 - a^2)^{1/3}[(1 + a)^{1/3} + (1 - a)^{1/3}]$$

$$g(a) \equiv \sqrt{(3a^2 + f(a)^2)}$$

スピンパラメータ(a)依存性:磁場増幅の時間スケール

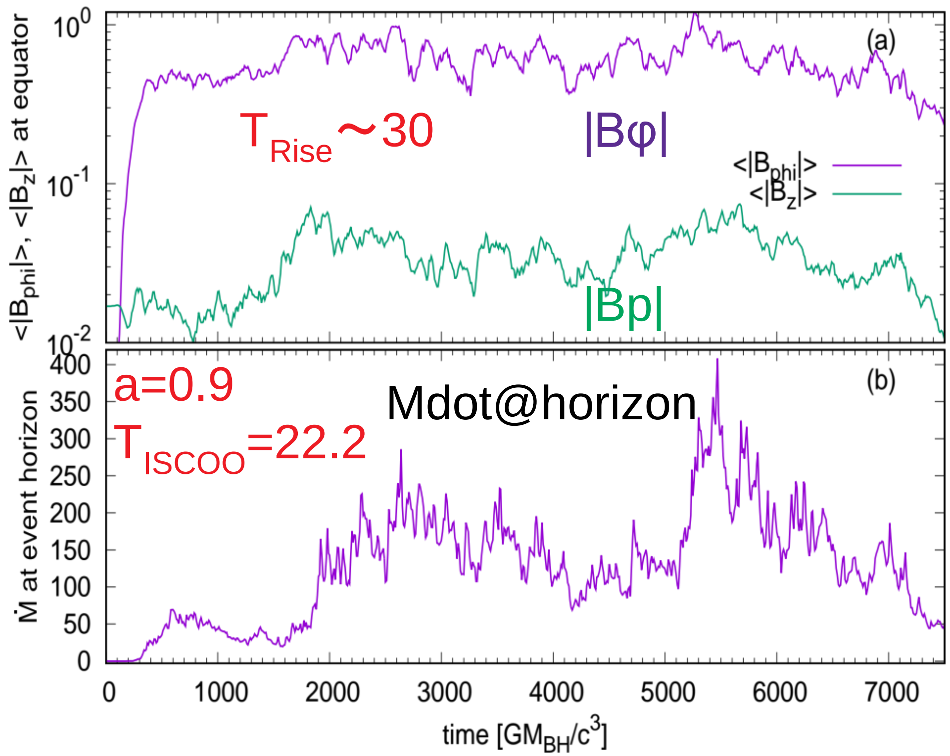

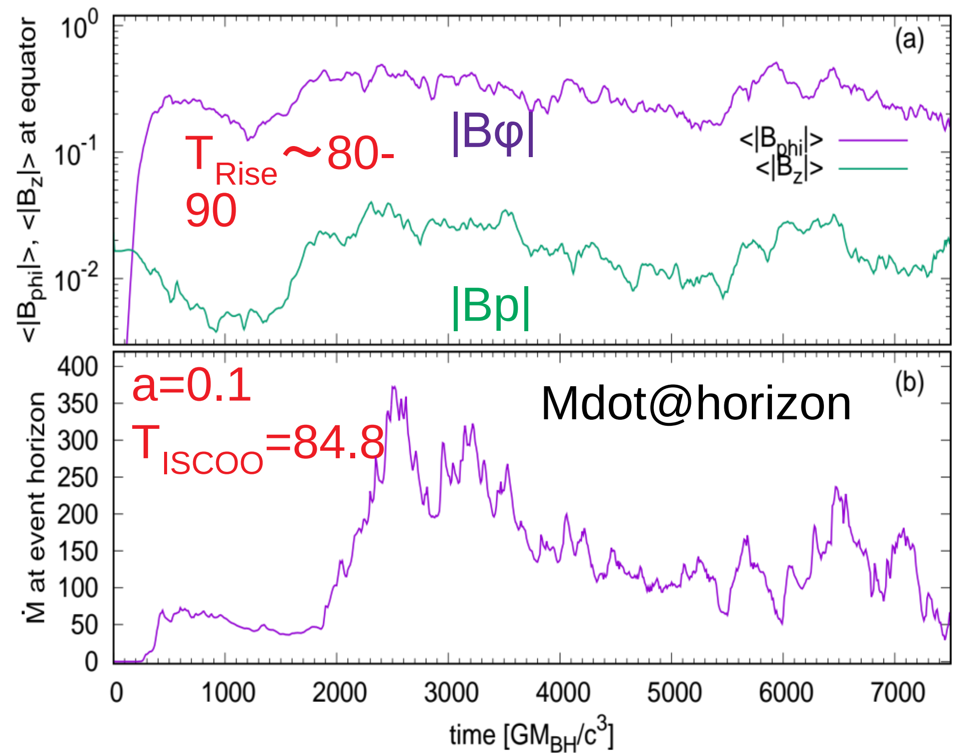

— スピンパラメータ a が小さくなるにつれ、磁場増幅、質量降着率の時間変動は長くなる

—その時間スケールは ISCO 半径のやや外側でMRIによる磁場増幅の最大成長率のモードの時間スケール程度

Butterfly diagram & EM jet power

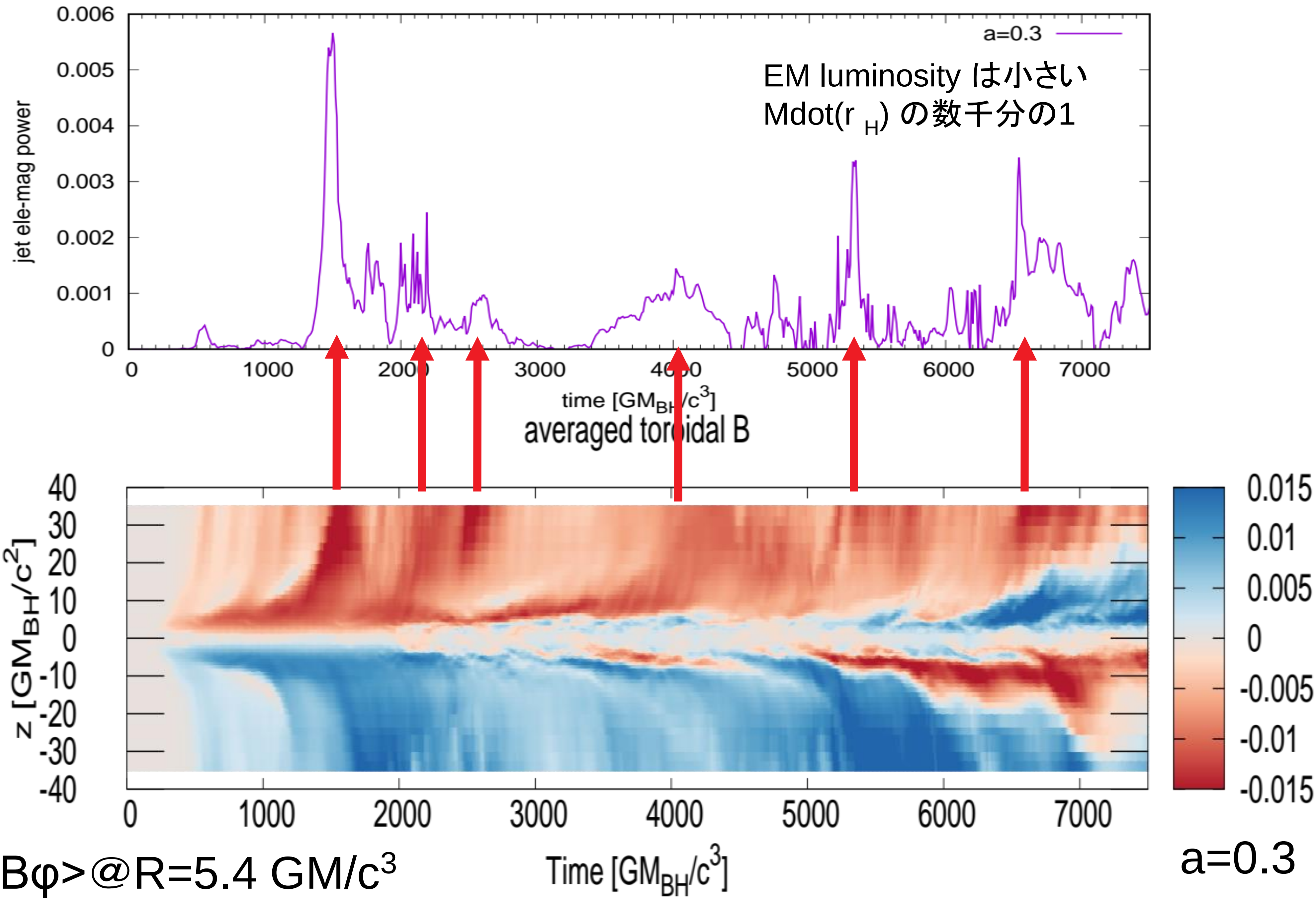

<Bφ>@R=5.4 GM/c^3

a=0.3

Pondermotive 力による粒子加速

– ジェット中に円盤の活動性を起源とする電磁フレア
– strength parameter a_0 at maximum peak in Alfven flare highly exceeds unity as estimated in Ebisuzaki & Tajima (2014);

$$a_0 = \frac{eE}{m_e \omega_A c} = 8.8 \times 10^{10} \left(\frac{M}{10^8 M_\odot} \right)^{1/2} \left(\frac{\dot{M}_{\rm av} c^2}{0.1 L_{\rm Ed}} \right)^{1/2}$$

– ジェットの密度が下がることによりAlfven wave＝>EM wave
Ponderomotive 力によって荷電粒子が加速される

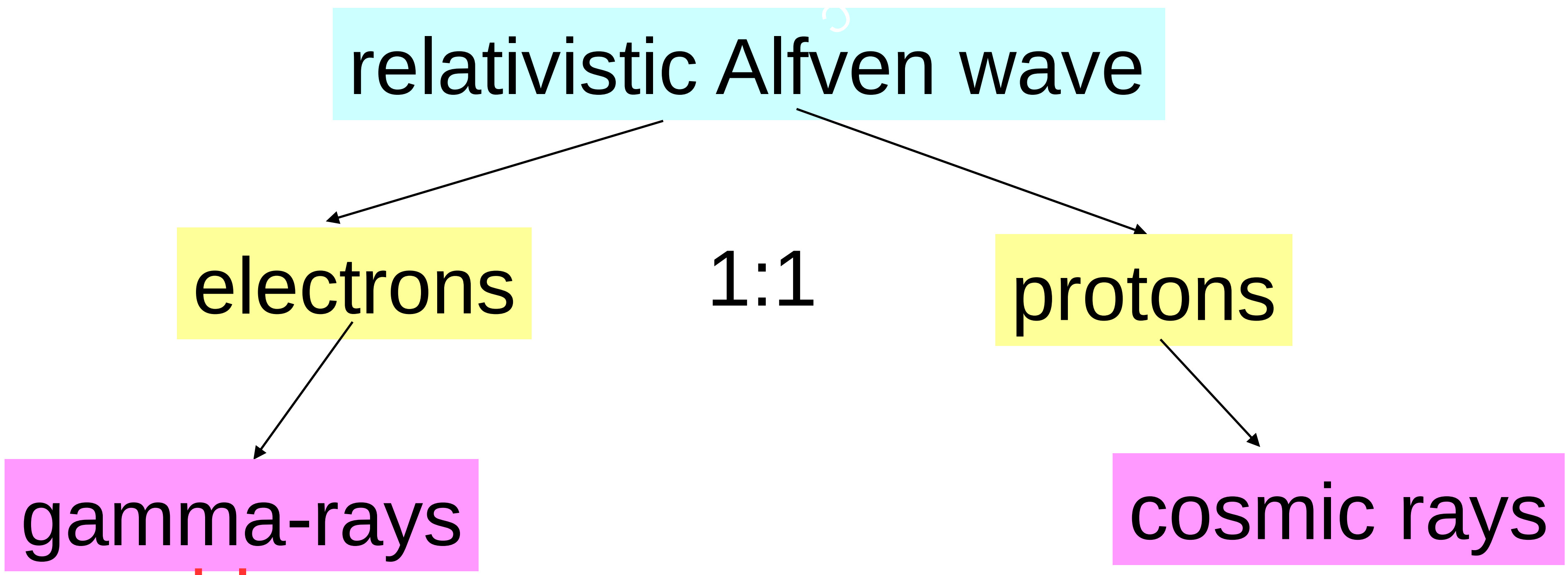

Ebisuzaki & Tajima 2014

フェルガンマ線観測衛星によるガンマ線フレア

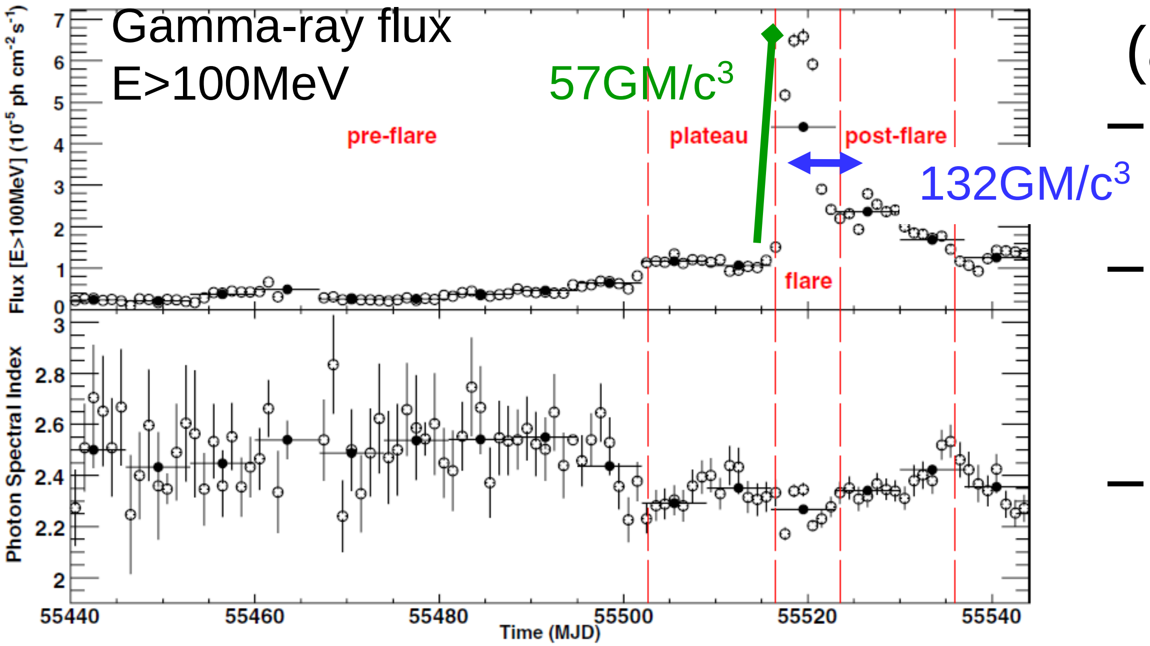

Fermi observation Abdo + ApJ 2010

– 相対論的アルフヴェン波の放射 ($a_0 \gg 1$)

– 電磁波モードへの変換

– べき的分布をする
加速された電子＋磁場

– シンクロトロン放射、
逆コンプトン放射(ガンマ線)

	our results	3C454.3	AO0235+164
rising timescale of flares ($\bar{\tau}_1$)	30	57^a	325^b
repeat cycle of flares ($\bar{\tau}_2$)	100	132^a	433^b

3C454.3 (M_{BH} ~$5 \times 10^8 M_{sun}$ Bonnoli et al. 2011)

まとめ

3D GRMHD simulations of rotating BH+accretion disk

– MRI による磁場増幅と磁気散逸に伴う時間変動
  ●カースピンパラメータ a が大きくなると
  時間変動小、jet のPoynting 光度大
– アルフヴェンパルスの放射
  ●赤道面付近での磁場の増幅期から散逸期
  ●円盤鉛直方向
  ●一部はジェットに伝わり、ポインティング成分の
  時間変動の起源に
  ●荷電粒子の加速(proton:UHECR, electron blazars)

今後　極軸付近を含めた高解像度計算

Wakefield acceleration (Tajima & Dawson PRL 1979)

Acceleration mechnism by interaction between wave and plasma.

図1−1

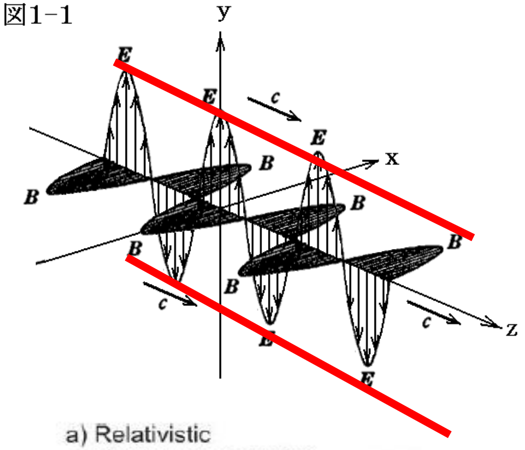

Laser plasma interaction
$\Rightarrow$ 8 shape motion.

$$\mathbf{F} = q\left(\mathbf{E} + \frac{\mathbf{v}}{c} \times \mathbf{B}\right)$$

Osillation by Electrifield $\Rightarrow$ **v (ossilation up, down)**
vxB force $\Rightarrow$ ossilation forward and backward.
|**v**| ~ c => large amplification motion by **vxB. (8 shape motion).**

If there is gradient in E^2, charged particles feel the force towars lees **E**^{2} side. = “Ponderamotive force”

Effective acceleration for I~10^{18}W/cm^2 (relativistic intensity). Experimentally observed.

Short pulse laser

grad **E**^{2}

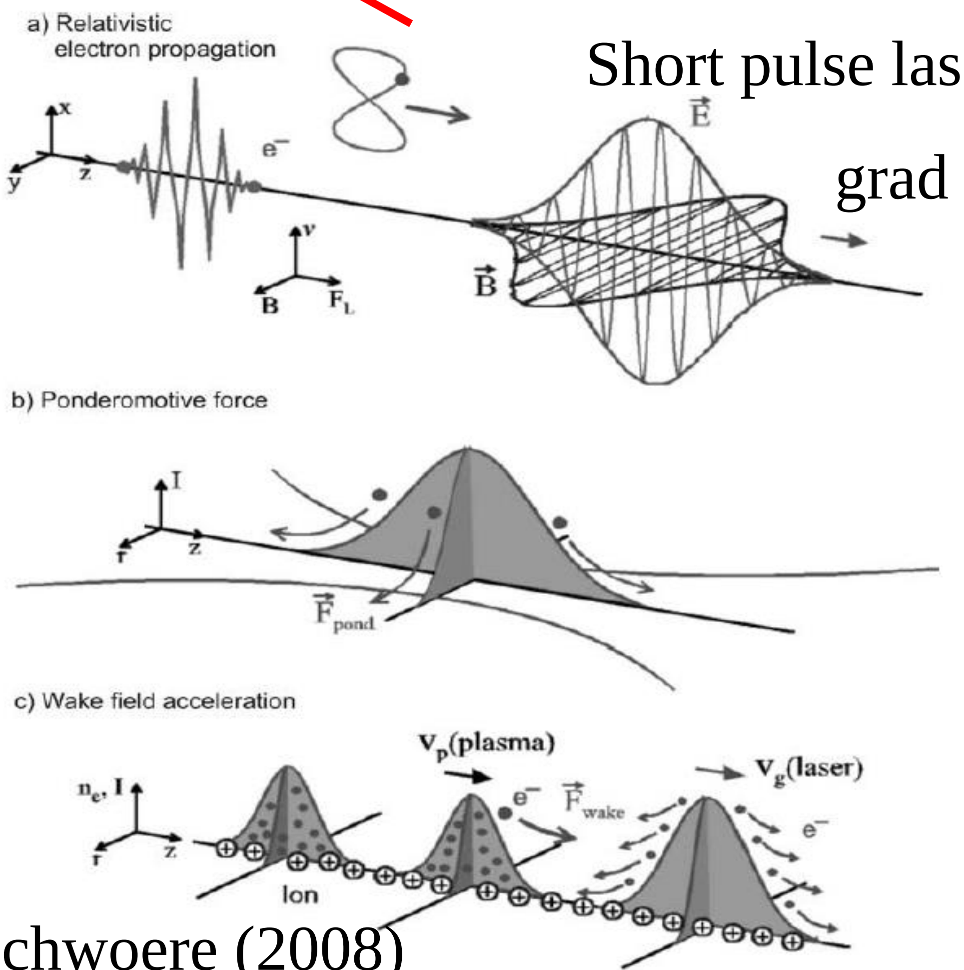

Schwoere (2008)

Relativistic Alfven wave can be applied to wakefield acceleration. (Takahashi+2000, Chen+2002, Lyubarusky 2006, Hoshino 2008)